Journal of the Taiwan Institute of Chemical Engineers 100 (2019) 47–55

Contents lists available at ScienceDirect

Journal of the Taiwan Institute of Chemical Engineers

journal homepage: www.elsevier.com/locate/jtice

Catalytic oxidation of various aromatic compounds in supercritical water: Experimental and DFT study

Bowen Yang[a], Zhiwen Cheng[a], Tao Yuan[a], Zhemin Shen[a,b,*]

[a] School of Environmental Science and Engineering, Shanghai Jiao Tong University, Shanghai, 200240, China
[b] Shanghai Institute of Pollution Control and Ecological Security, Shanghai, 200092, China

ARTICLE INFO

Article history:
Received 13 September 2018
Revised 21 December 2018
Accepted 2 February 2019
Available online 11 May 2019

Keywords:
Aromatic compounds
Catalytic supercritical water oxidation (CSCWO)
Bisphenol A (BPA)
$Cu(NO_3)_2$

ABSTRACT

Catalytic supercritical water oxidation (CSCWO) has sprung up as a promising technique to eliminate refractory aromatic compounds, which are difficult to be removed by conventional wastewater treatment processes. Decompositions and degradation mechanisms of 18 aromatic compounds, including benzene, phenol, bisphenol A (BPA) *etc.*, were investigated using CSCWO in this study. It was found that TOC removal efficiencies of the aromatic compounds were significantly enhanced, when CSCWO temperatures raised from 325 to 525 °C and reaction time prolonged from 0.5 to 6 min, with the addition of $Cu(NO_3)_2$. The correlationships among TOC degradation rates (k_{TOC}), temperature at TOC removal rate of 90% (T_{90}) and 19 molecular descriptors were studied. The results indicated that BO_n and $q(H)_x$ could greatly impact the degradation behaviors. Fukui indices based density functional theory (DFT) method was applied to reveal the conceivable degradation pathway of BPA during CSCWO process.

1. Introduction

As a group of refractory environmental pollutants, aromatic compounds have high toxicity and poor biodegradability, resulting in both environmental and human health problems [1–4]. Among aromatic compounds, benzene, phenols and toluene are often regarded as hazardous matters due to highly potential carcinogenicity [5,6]. Bisphenol A (BPA), nonylphenol (NP) and octylphenol (OP), as kinds of endocrine disrupting chemicals (EDCs), could simulate the hormones and disturb endocrine system even under trace concentrations [7–9]. Owning to possessing benzene ring, aromatic compounds are persistent, as a result, they are difficult to be removed completely by traditional wastewater treatment processes, like activated sludge and biodegradation [10,11]. To resolve the intractable problem, supercritical water oxidation (SCWO) has been considered as a high-effective process for treating toxic and bio-refractory wastes in recent decades [12,13]. It was believed that above the supercritical water point (temperature= 374 °C, pressure= 22.1 MPa), organic compounds and oxygen gas would become soluble, and then a fast reaction happened within a single phase, which resulted that refractory organics could be successfully mineralized into CO_2, H_2O, N_2 and few inorganic salt within seconds or minutes [12,14].

In order to lower severe experimental temperatures and pressure requirements, as well as obtain better removal efficiencies, catalytic supercritical water oxidation (CSCWO) has been proposed in recent decades. Catalysts, like Cu(II), Co(II), Ni(II), Mn(II), Zr(IV), Zn(II), Ti(IV), Ce(IV), have been widely used into CSCWO researches [15–20]. Dong et al. investigated catalytic and non catalytic supercritical water oxidation of p-nitrophenol, the result showed that the reaction rate in catalyst MnO_2 process was much higher than that in non catalystic process [21]. Furthermore, Shin et al. explored CSCWO of acrylonitrile using $Ca(NO_3)_2$ and $Ca(OH)_2$, the result indicated that 94% carbon and 95% reactive nitrogen of acrylonitrile were converted into $CaCO_3$ and N_2. Meanwhile, the in situ formed $CaCO_3$ could act as a catalyst to facilitate acrylonitrile degradation [22].

Nevertheless, the aforementioned works merely focused on one or few target compounds. To the best of our knowledge, data is still sparse on CSCWO of a series of aromatic compounds, especially for EDCs. In addition, density functional theory (DFT) is an attractive method for revealing reaction mechanism from the aspect of quantum chemistry, which has resoundingly elucidated many experimental phenomena [23–25]. Previously, we have investigated SCWO of dozens of organic compounds, and observed that some molecular characteristics, *e.g.* dipole moment and Fukui indices, could take an important role in destroying the organics during SCWO process without catalysts [26–28]. As a result, this work aims to explore the effect of catalysts on decomposition of aromatic compounds during SCWO. The catalysts

* Corresponding author at: School of Environmental Science and Engineering, Shanghai Jiao Tong University, Shanghai, 200240, China.
E-mail addresses: shenzhemin@sina.com.cn, shenzhemin@sina.com (Z. Shen).

https://doi.org/10.1016/j.jtice.2019.02.002
1876-1070/

Table 1
Information of 18 aromatic compounds.

Compounds	Abbreviation	Molecular formula	CAS No.
Aniline	Aniline	C_6H_7N	62–53–3
Nitrobenzene	NB	$C_6H_5NO_2$	98–95–3
Quinoline	Quinoline	C_9H_7N	91–22–5
Potassium hydrogen phthalate	KHP	$C_8H_5KO_4$	877–24–7
Phthalic anhydride	PA	$C_8H_4O_3$	85–44–9
2,7-dihydroxynaphthalene	2,7-PADN	$C_{10}H_8O_2$	582–17–2
Benzene	Benzene	C_6H_6	71–43–2
Phenol	Phenol	C_6H_6O	108–95–2
Catechol	Catechol	$C_6H_6O_2$	120–80–9
Phloroglucinol	1,3,5-THB	$C_6H_6O_3$	108–73–6
Methylbenzene	MB	C_7H_8	108–88–3
2-cresol	2-cresol	C_7H_8O	1319–77–3
2,4-dichlorophenol	2,4-DCP	$C_6H_4Cl_2O$	120–83–2
Benzenesulfonic acid	BSA	$C_6H_6O_3S$	98–11–3
3-phenylpropionic acid	3-PPA	$C_9H_{10}O_2$	501–52–0
Bisphenol A	BPA	$C_{15}H_{16}O_2$	80–05–7
Nonylphenol	NP	$C_{15}H_{24}O$	84,852–15–3
Octylphenol	OP	$C_{14}H_{22}O$	140–66–9

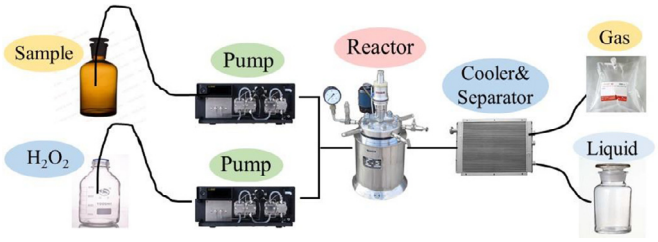

Fig. 1. Scheme of SCWO apparatus.

were divided into three parts: (1) different cations, like $Cu(NO_3)_2$, $Fe(NO_3)_3$, $Mn(NO_3)_2$, $Zn(NO_3)_2$, $AgNO_3$, $Ni(NO_3)_2$, $Zr(NO_3)_4$ and $Ce(NO_3)_3$; (2) different anions, such as $CuSO_4$, $CuCl_2$, $Cu(NO_3)_2$, as well as $ZnSO_4$, $ZnCl_2$, $Zn(NO_3)_2$; (3) different heteropolyacid catalysts, *e.g.* phosphotungstic acid ($H_3PW_{12}O_{40}$, PTA), tungstosilicic acid ($H_4SiW_{12}O_{40}$, TSA) and phosphomolybdic acid ($H_3PMo_{12}O_{40}$, PMA). Besides, DFT method was applied to calculate the quantum properties of the 18 aromatic compounds to further reveal the correlation between TOC removal and molecular structural parameters.

2. Experimental

2.1. Apparatus and experimental procedures

The experimental apparatus has been fully described in our previous work, investigating the reaction time affecting the SCWO of N-containing compounds [28]. In brief, the reactor is made of Hastelloy alloy, whose designed an effective volume of 10 mL and the maximum operating pressure and temperature are 40 MPa and 600 °C, respectively (Fig. 1). It should be noted that all experiments in this work were performed at a constant pressure of 24 MPa, temperature and reaction time were designed as 325, 375, 425, 475 and 525 °C, as well as 0.5, 1, 1.5, 3 and 6 min, respectively.

2.2. Materials and analytical methods

The information of 18 aromatic compounds was shown in Fig. 2 and Table 1. The initial concentration was 1 mM for most of target compounds, however, the saturated solubility of certain compounds, like OP and NP, was under 1 mM, then the saturated solution of these ones was applied to perform the experiments. The saturated solution was achieved as the following steps. Firstly, the sample was prepared with 1 mM initial concentration of the poor solubility target compound. Secondly, after 12 h of magnetic stirring at a constant temperature of 25 °C, the sample was filtered through 1.2 μm glass fiber filter, which had been washed by ultrapure water before filtration, in order to avoid interference. Moreover, in order to avoid causing problematic corrosion and precipitation, the initial concentration of the catalysts was 0.02 mM based on the transition metal ion, for example 0.02 mM for $Fe(NO_3)_3$, 0.00167 mM for PTA, TSA and PMA. Considering the initial concentration was as low as 1 mM or even less, 300% excess oxygen was used into this study to keep sufficient oxidation.

The information of quantum parameters used in this work was listed in Table 2. Quantum parameters of the 18 aromatic compounds were calculated using Gaussian 09 (DFT B3LYP/6–311 G level) and Material Studio 6.1 (Dmol3/GGA-BLYP/DNP(3.5) basis). The aromatic compounds' structures were optimized by DFT B3LYP/6–311 G method via Gaussian 09 at first. Then the exchange, correlation terms and natural population analysis of atom charge were calculated by B3LYP function. The maximum displacement, maximum force, maximum iterations and convergence tolerance were set as 0.005 Å, 0.002 Ha/Å, 500 and 1×10^{-5} Ha, respectively. Moreover, the density mixing and self-consistent field were set as 0.2 charge with 0.5 spin and 10^{-6} a.u., respectively [29,30]. Finally, according to the abovementioned methods, the molecular characteristics were achieved from the outmol file, which included dipole moment (μ), most positive partial charge on a hydrogen atom $(qH)_x$, most negative or positive partial charge on a carbon atom $(q(C)_n/q(C)_x)$, most negative or positive partial charge of a hydrogen atom connected to a carbon atom $(q(C–H)_n/q(C–H)_x)$, minimum and maximum number of chemical bonds between a pair of coterminous atoms (BO_n/BO_x), energy of highest occupied molecular orbital (E_{HOMO}), energy of the lowest unoccupied molecular orbital (E_{LUMO}) and energy of molecule calculated by B3LYP method (E(B3LYP)). Besides, Fukui indices, as the key descriptors, were choosed to predict the site reactive selectively between the reaction pathways. For example, $F(+)_x$, $F(-)_x$ and $F(0)_x$ stand for the maximum values of nucleophilic attack, electrophilic attack and ·OH radical attack, respectively, meanwhile $F(+)_n$, $F(-)_n$ and $F(0)_n$ represent their respective minimum values on main-chain carbon atom. These parameters were successfully conducted into our previous research [27].

Total organic carbon (TOC) was measured by the TOC-Analyzer (Multi N/C 3000, Analytik Jena AG, Jena, Freistaat Thüringen, Germany) under burning temperature of 850 °C with CeO_2. Moreover, TOC removal rate was defined as follows:

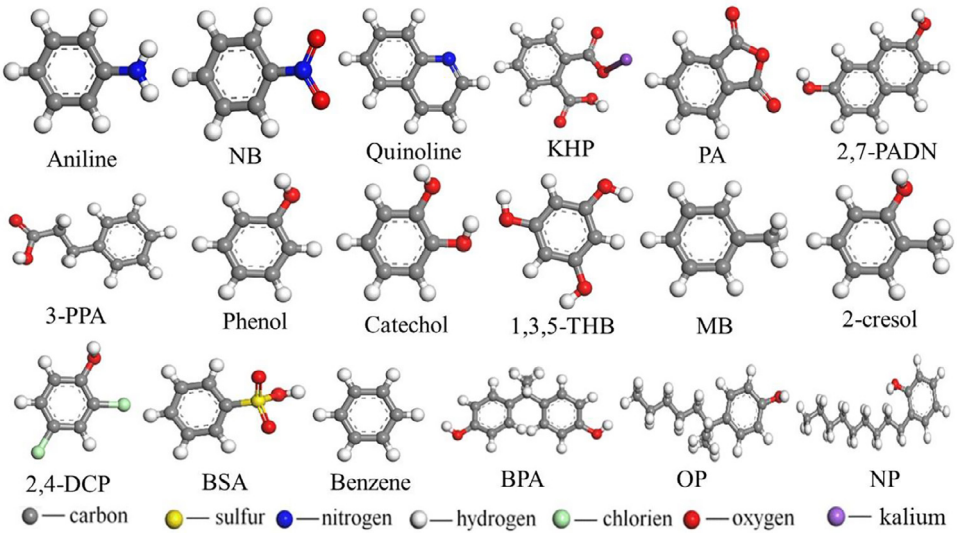

Fig. 2. Structural formula of 18 aromatic compounds.

Table 2
Information of nineteen quantum parameters.

Descriptors	Interpretation
μ	Dipole moment
E_{B3LYP}	The total energy of a molecule
E_{HOMO}	Energy of the highest occupied molecular orbital
E_{LUMO}	Energy of the lowest unoccupied molecular orbital
E_{GAP}	The gap energy ($E_{LUMO}-E_{HOMO}$)
E_{SUM}	The sum energy ($E_{LUMO}+E_{HOMO}$)
$q(H)_x$	Most positive partial charge on a hydrogen atom
$q(C)_n/q(C)_x$	Minimum and maximum negative partial charge on a carbon atom
$q(C-H)_n/q(C-H)_x$	Minimum and maximum positive partial charge on a hydrogen atom linked with a carbon atom
BO_n/BO_x	Minimum and maximum number of chemical bonds between a pair of coterminous atoms
$F(0)_n/F(0)_x$	Minimum and maximum value of Fukui indices by hydroxyl radical attack
$F(+)_n/F(+)_x$	Minimum and maximum value of Fukui indices by nucleophilic attack
$F(-)_n/F(-)_x$	Minimum and maximum value of Fukui indices by electrophilic attack

$$\text{TOC removal efficiency} = \left(1-\frac{concentraion\ of\ TOC\ in\ the\ effluent}{concentration\ of\ TOC\ in\ the\ initial\ concentration}\right)\times 100\%$$

3. Results and discussion

3.1. Effect of different catalysts

KHP has a wide range of applications in many research areas, because it is commonly used as a primary standard for calibrating TOC analyzer and pH-meters. Therefore, KHP was chosen as a representative compound in exploring the effect of different catalysts during SCWO process. As shown in Fig. 3a, it was obvious that compared with non catalytic reaction, all the cation catalysts, such as Cu(II), Mn(II), Zn(II), Ni(II), Ag(I), Fe(III), Ce(III) and Zr(IV), could improve TOC removal. The results were in agreement with previous study, Park et al. investigated CSCWO of wastewater containing terephthalic acid and found that the addition of catalysts, such as MnO_2, Al_2O_3 and CuO, could effectively improve COD conversion. However, the COD conversion rate had a huge difference between 19% and 98%, this might come from different operating parameters, like temperature, pressure and oxygen concentration, as well as different catalysts [31].

Among the cations, Cu^{2+} achieved the best TOC removal during CSCWO process. Similar results were found in previous studies, Zhang et al. examined wet oxidation of sewage sludge using metals ions, like Cr^{3+}, Cu^{2+}, Fe^{3+}, Zn^{2+} and Mn^{2+}, the optimal result demonstrated that at the condition of 240 °C and 60 min, Cu^{2+} took a more significant part than the others [32]. Based on related studies, the catalysis oxidation pathway could be interpreted as below [33,34]:

$$Cu^{2+} + H_2O_2 \rightarrow Cu^{+} + H^{+} + HO_2 \quad (R1)$$

$$Cu^{+} + H_2O_2 \rightarrow Cu^{2+} + OH^{-} + \cdot OH \quad (R2)$$

Cu^{2+} could react with H_2O_2 and form Cu^{+}, which could facilitate the formation of hydroxyl radical (·OH) from H_2O_2. Due to ·OH had high-effective oxidation, as a result, it could oxidize the target compound. Qi et al. studied decomposition of aniline in CSCWO, and found that ferrous ions could react with H_2O_2, which resulted in the generation of ·OH [16]. Similarly, Kosari et al. examined CSCWO of tributhyl phosphate using Ag_2O, CuO, Fe_2O_3, MgO and ZnO nanoparticles, the result showed that activated oxygen would be produced from supercritical water in the presence of a catalyst [35].

To explore the effect of heteropolyacid catalysts on TOC removal, PTA, TSA and PMA were conducted into this work. In Fig. 3b, comparison of non-catalyst, the addition of PTA, TSA and PMA achieved higher TOC removal, which implied that heteropolyacid catalysts could effectively improve TOC removal during SCWO process. Similarly, Arslan and Ferry used TSA as the catalyst to investigate SCWO of nitrobenzene (NB), the result showed the decomposition of NB could be largely improved under the presence of TSA [36]. Besides, TOC removal efficiency generally followed

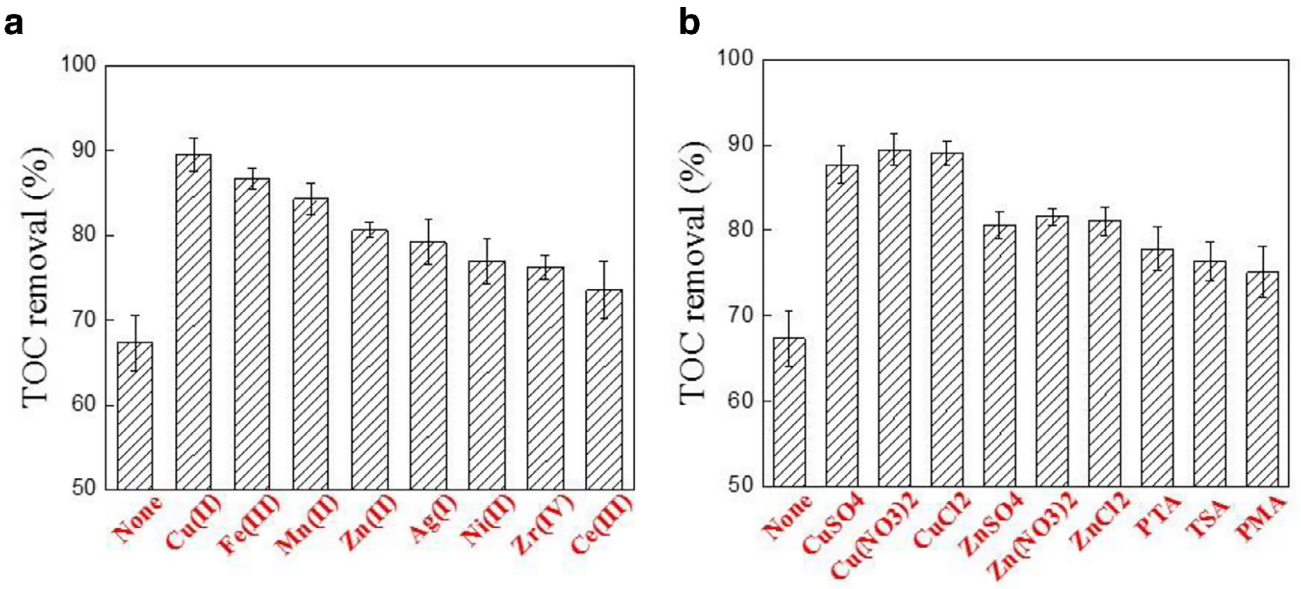

Fig. 3. TOC removal under various catalysts (425 °C, 24 MPa and 1 min). (a) for different cations, such as $Cu(NO_3)_2$, $Fe(NO_3)_3$, $Mn(NO_3)_2$, $Zn(NO_3)_2$, $AgNO_3$, $Ni(NO_3)_2$, $Zr(NO_3)_4$ and $Ce(NO_3)_3$. (b) for different anions and heteropolyacid catalysts, like $CuSO_4$, $Cu(NO_3)_2$, $CuCl_2$, $ZnSO_4$, $Zn(NO_3)_2$, $ZnCl_2$ as well as PTA, TSA and PMA.

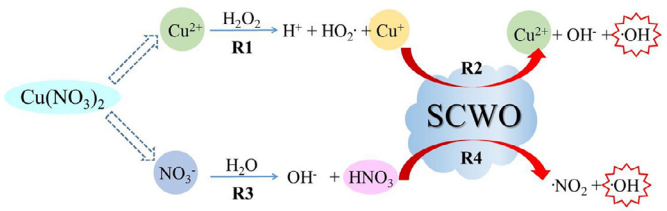

Fig. 4. The conceivable catalysis oxidation mechanism of $Cu(NO_3)_2$.

the order that PTA > TSA > PMA in this work. Moreover, different anions, like SO_4^{2-}, NO_3^- and Cl^-, were also investigated. From Fig. 3b, NO_3^-obtained a slightly higher TOC removal efficiency than SO_4^{2-} and Cl^-. There were some researches verified that nitrate could participate in oxidizing the target compounds during SCWO, because $NO_3^-$was supposed to be an effective oxidizing agent [37]. Some researchers proposed the reaction scheme (R3-R4), firstly, the nitrate could react with H_2O and formed HNO_3 [38]. Secondly, HNO_3 could generate HO· and ·NO_2 radicals by hydrolysis. Finally, ·NO_2 could oxidize the organic compound and reduced into N_2 [39]. Based on the facts examined above, a conceivable catalysis oxidation mechanism of $Cu(NO_3)_2$ was proposed in Fig. 4. In brief, $Cu(NO_3)_2$ could form Cu^{2+} and NO_3^-, then on the one hand Cu^{2+} had a catalytic impact in SCWO process, and facilitated the generation of ·OH from H_2O_2. On the other hand, NO_3^- could react with H_2O and produced HNO_3, then it generated ·OH and ·NO_2 via hydrolysis. Additionally, in case of $Cu(NO_3)_2$ and $CuCl_2$, the TOC removal had not considerable difference. It was well accepted that Cl atom would be converted into HCl during SCWO. HCl, as a strong acid, could corrode the Hastelloy alloy reactor walls and then transition metal ions, such as Ni^{3+}, Fe^{3+}, $Mn^{2+}$and Cu^{2+}, would be produced, which might play a positive role on TOC removal. Similar results were found in the previous study, Hatakeda et al. investigated corrosion on continuous SCWO for polychlorinated biphenyls, the result showed that the Hastelloy alloy was proved to be corroded on the surface located between the bottom of the reactor and cooling parts [40].

In sum, $Cu(NO_3)_2$ obtained the best TOC removal among all the catalysts. As a result, $Cu(NO_3)_2$ was chosen as the catalyst and brought into later study.

$$NO_3^- + H_2O \leftrightarrow OH^- + HNO_3 \quad \text{(R3)}$$

$$HNO_3 \leftrightarrow HO\cdot + \cdot NO_2 \quad \text{(R4)}$$

3.2. Effect of temperature

As shown in Fig. 5, TOC removal efficiencies of 18 aromatic compounds had a sharp increase as temperature ranged from 325 to 525 °C. Except for benzene, the other target compounds achieved more than 90% TOC removal efficiencies after 525 °C. Similar results were found in previous works, Dong et al. investigated CSCWO of 4-nitrophenol and observed that the removal efficiency was near 100% when temperature increased from 380 to 440 °C with the addition of MnO_2/Ti-Al oxide [21]. Angeles–Hernández choosed MnO_2/CuO as catalyst and studied the destruction of quinoline during CSCWO, the result indicated TOC removal rate of quinoline was more than 90% as temperature was above 500 °C [41]. In this work, quinoline achieved near 100% of TOC removal rate after 475 °C.

Furthermore, it was important to note that when temperature was up to 525 °C, the TOC removal efficiencies of BPA, NP and OP were near 100%, which indicated that EDCs could be successfully mineralized during catalytic supercritical water oxidation. However, in terms of BPA, NP and OP, data is still sparse on the decomposition of EDCs during CSCWO process, based on other related AOPs studies, Gao et al. examined the degradation of BPA using transition metals activating persulfate process, and found BPA could be removed more than 90% with the presence of Fe^{2+} or NiO_3 after 30 min at normal atmospheric temperature [42]. Potakis et al. investigated oxidation of BPA in water by heat-activated persulfate, the result showed that activation temperature increased from 40 to 70 °C could lead to the removal efficiencies of BPA raised from 10% to 100% within 5 min, which resulted in an 80-fold degradation rate increase [43]. Compared with these results, TOC removal efficiencies of EDCs in this work were near 100% within 1.5 min, which implied CSCWO was a time-saving and high-effective process for removing EDCs.

3.3. Effect of reaction time

TOC removal efficiencies of 18 aromatic compounds under different reaction times with a constant temperature of 425 °C were

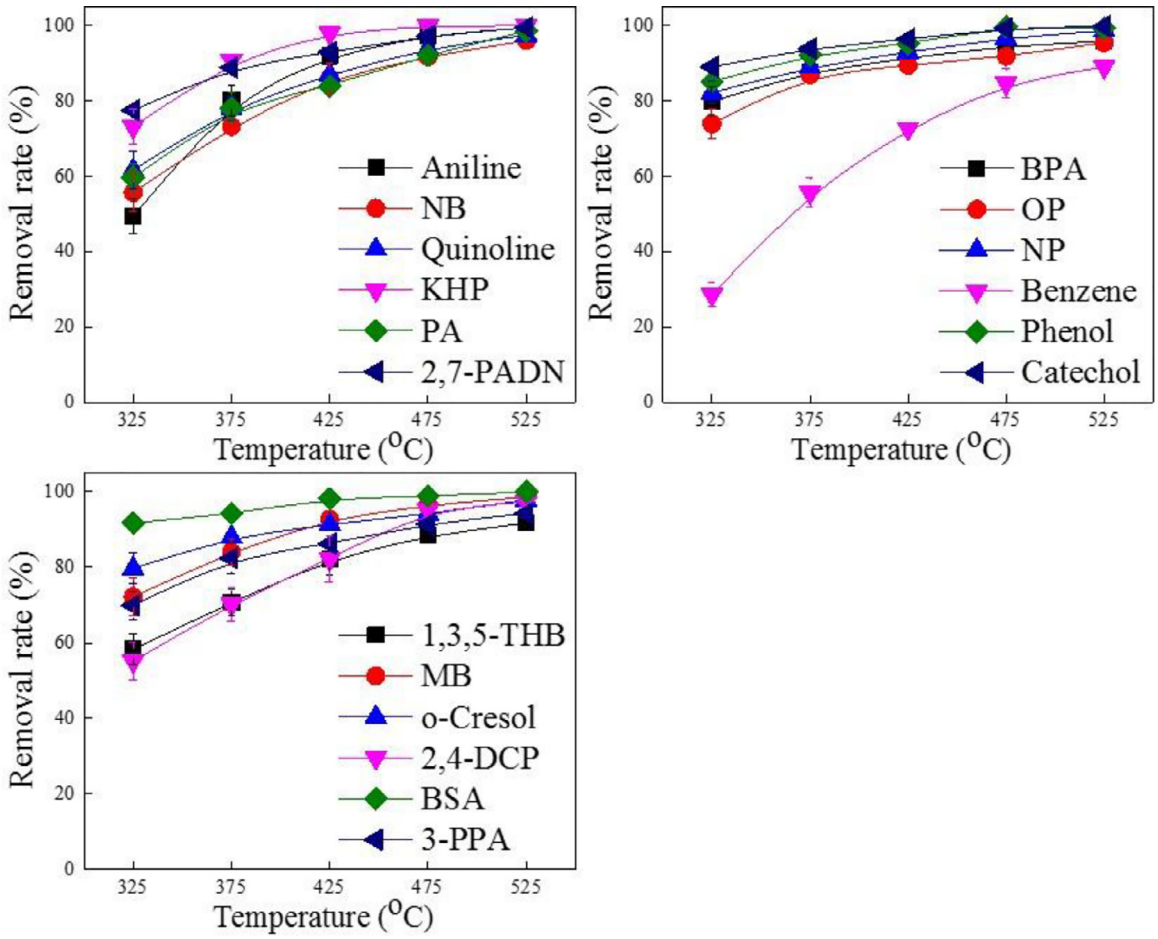

Fig. 5. TOC removal under various temperatures with a constant reaction time and pressure of 1.5 min and 24 MPa, respectively, as well as 0.02 mM $Cu(NO_3)_2$.

presented in Fig. 6. The TOC removal rates raised largely as reaction time prolonged from 0.5 to 1.5 min, then the growth tended to be steady after 3 min, finally all the target compounds obtained over 90% of TOC removal rates at 6 min. The results were also in agreement with the previous study, Tan et al. investigated SCWO of 12 organics, including aniline, nitrobenzene, phenol and BSA, the result indicated that the TOC concentrations became to none when reaction time raised from 140 to 460 s under temperature over 450 °C [26]. Yang et al. examined the decomposition of 41 nitrogen-containing compounds, including aniline and NB, during SCWO, and observed the TOC removal efficiencies of most compounds were above 80% and even to 100% when reaction time raised from 0.5 to 6 min [28].

3.4. TOC degradation rates

Lots of studies presented that a pseudo-first-order kinetic model could successfully illustrate the macro-kinetics for SCWO of wastes [44–47]. Therefore, to further compare the decomposition difference between the 18 target compounds, the TOC degradation rates (k_{TOC}) had been calculated via a pseudo-first-order kinetic model, as followed:

$$\ln([TOC]_0/[TOC]_t) = k_{TOC}t$$

where $[TOC]_0$ stood for the initial TOC concentration of each compound, $[TOC]_t$ indicated its TOC concentration at time t, k_{TOC} represented the TOC degradation rate constants of each compound, t was the reaction time. As a result, the TOC degradation rate constants (k_{TOC}) of 15 target compounds had been presented in Table 3.

Table 3
The TOC degradation rates of 18 aromatic compounds in CSCWO (0.5–6 min, 425 °C and 24 MPa).

Compound	k_{TOC} (min $^{-1}$)
Aniline	1.682
NB	1.465
Quinoline	1.423
Benzene	0.855
MB	1.822
Phenol	2.031
Catechol	2.264
1,3,5-THB	1.197
2-Cresol	1.730
2,4-DCP	1.194
BSA	2.731
KHP	2.439
PA	1.428
2,7-PADN	1.797
3-PPA	1.542
BPA	1.665
OP	1.576
NP	1.858

As shown in Table 3, it was clear that the TOC degradation rates were in an order that BSA (2.731) > KHP (2.439) > catechol (2.264) > phenol (2.031) > NP (1.858) > MB (1.822) > 2,7-PADN (1.797) > 2-cresol (1.730) > Aniline (1.682) > BPA (1.665) > OP (1.576) > 3-PPA (1.542) > NB (1.465) > PA (1.428) > Quinoline (1.423) > 1,3,5-THB (1.197) > 2,4-DCP (1.194) > benzene (0.855). There was a huge difference of TOC degradation rates between 18

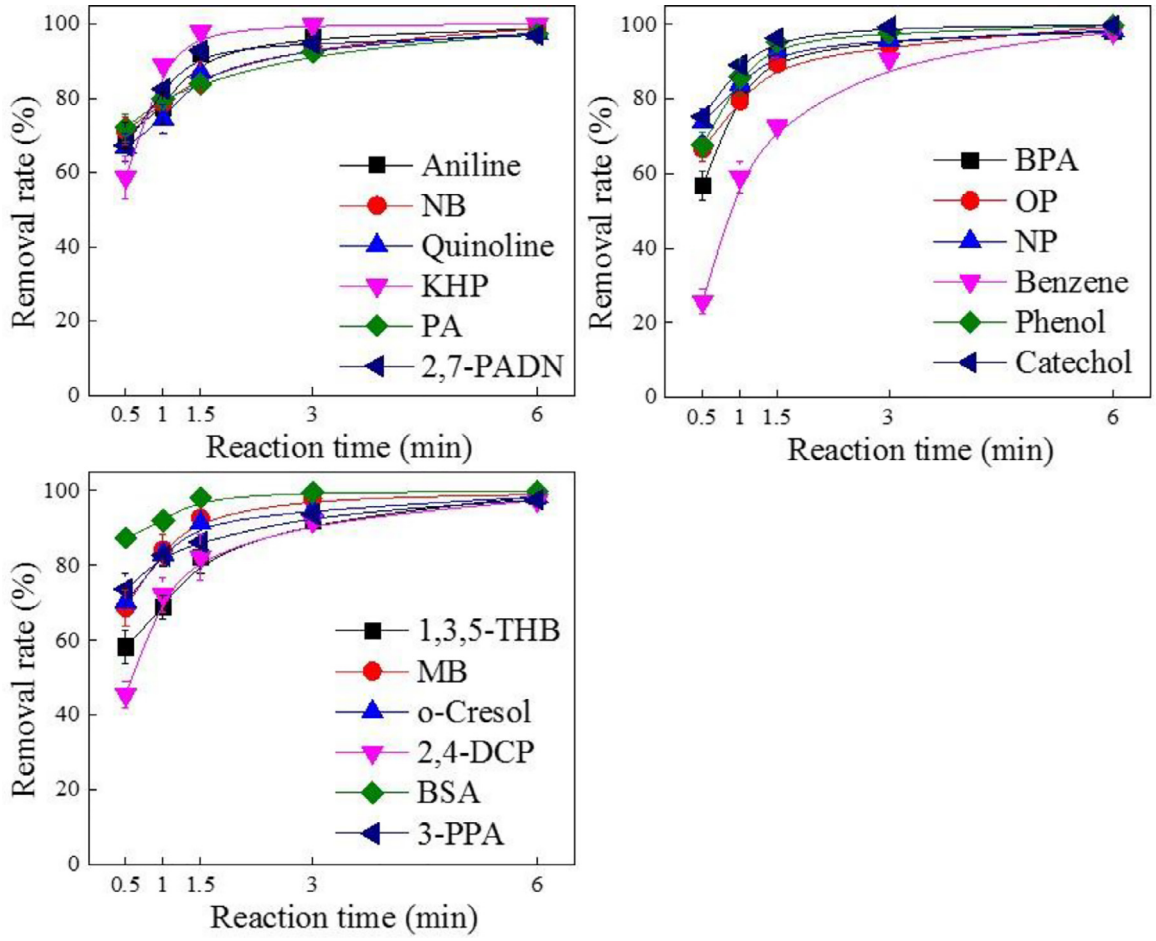

Fig. 6. TOC removal under various reaction times with a constant temperature and pressure of 425 °C and 24 MPa, respectively, as well as 0.02 mM $Cu(NO_3)_2$.

aromatic compounds, which might come from the various molecular parameters of each compound. As for phenol, there were some evidence showed that its kinetic constants were in a wide range of 0.345 to 4.275 min^{-1}, due to different non-isothermal reactors, reactor material, initial concentrations, experimental pressures and temperatures [48–50]. Besides, Kosari et al. explored CSCWO of tributhyl phosphate, the result indicated that under non-catalytic and catalytic conditions, the reaction kinetic constants were 0.008–0.027 min^{-1} and 0.014–0.034 min^{-1}, respectively, with temperature ranging from 370 to 480 °C [35].

3.5. Correlation analysis of k_{TOC}, T_{90} and molecular descriptors

Commonly, TOC was considered to be efficiently removed as the removal efficiency reached 90%. According to Fig. 5, the temperature at TOC removal efficiency of 90% (T_{90}) was achieved. All the 18 aromatic compounds' TOC degradation rates (k_{TOC}), T_{90} and their respective quantum parameters were shown in Table S1. The correlation coefficients indicated that μ, $q(H)_x$, $q(C–H)_x$, $q(C)_x$, E_{HOMO}, E_{SUM}, $F(-)_x$, $F(0)_x$ and BO_x were positively correlated to k_{TOC}, while E_{B3LYP}, $q(C–H)_n$, $q(C)_n$, E_{LUMO}, E_{GAP}, $F(+)_n$, $F(+)_x$, $F(-)_n$, $F(0)_n$, $F(0)_x$ and BO_n were negatively correlated to k_{TOC}. In terms of T_{90}, on the contrary, molecular descriptors, like μ, $q(H)_x$, $q(C–H)_x$, $q(C)_x$, E_{HOMO}, E_{SUM} and $F(-)_x$ were negative correlated, while E_{B3LYP}, $q(C–H)_n$, $q(C)_n$, E_{LUMO}, E_{GAP}, $F(+)_n$, $F(+)_x$, $F(-)_n$, $F(0)_n$, $F(0)_x$, BO_n and BO_x were positive correlated. It was understandable that for the same compound, if its k_{TOC} was large, which meant it could be removed easily, as a result it would also be degraded at a low temperature. In other words, the larger value of k_{TOC} was, the fewer value of T_{90} was.

Among all the parameters, it was BO_n that could play a most important role in affecting k_{TOC} and T_{90} during CSCWO process. Bond order (BO) represented the number of chemical bonds between a pair of atoms, giving an indication of the stability for a bond. From Table S1, all aromatic compounds' BO was less than 2. Generally, the less BO value was, the more easily to be attacked and resulted in bond breaking [51,52]. Another significant descriptor was $q(H)_x$, which reflected the most positive partial charge on a hydrogen atom. There is a general consensus that the more q(H) value was, the easier H atom could lose, which resulted in higher k_{TOC} constant. Besides, the molecular characteristic μ was the meaning of dipole moment, which stood for the polarity and charge separation in a molecule [53]. A compound with large μ value frequently resulted in the stronger electronegativity than that of small μ value. Therefore, in terms of those compounds with large μ value, it was more easily to accept the electrons from the oxidants, like ·OH, which resulted in a positive relationship with k_{TOC} values. The parameter $F(-)_n$ represented the minimum value of Fukui indices by electrophilic attack. $F(-)_n$ gave some information on site reactivity and could predict which region of a compound would be better prepared to donate charge [54]. It indicated that the electrophilic reaction dominates the removal of aromatic compounds during CSCWO process. These results were also in agreement with previous works, Cheng et al. revealed the relationship between reaction rate constant and quantum parameters in Fenton oxidation process, and proposed the main descriptors governing reaction rate were $q(H)_x$, $q(C–H)_x$ and $q(C–H)_n$, which were relevant

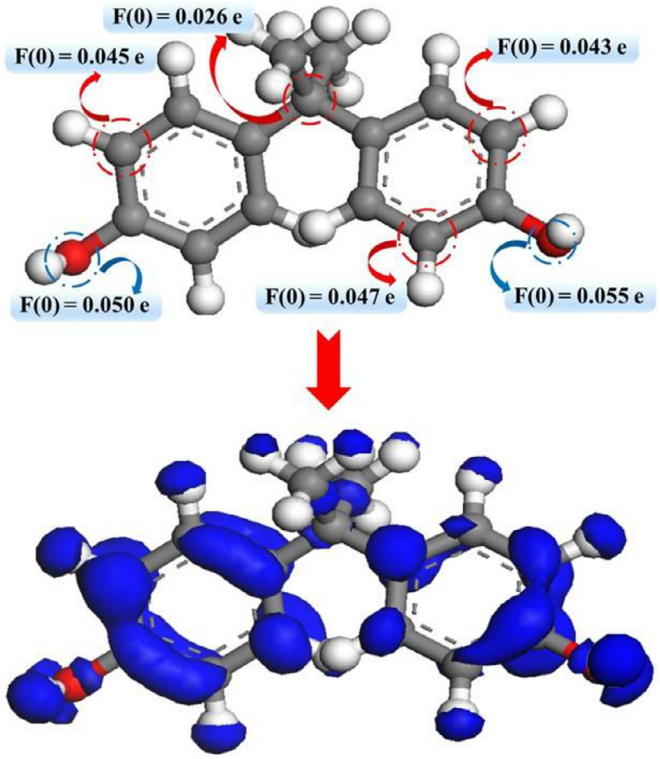

Fig. 7. Structural formula and Fukui function map with indices values of BPA.

to the active site and ·OH attack [55]. Similarly, Su et al. investigated the removal rates of organic pollutants by adsorption of manganese dioxide under acid condition, the result showed that $q(H)_x$, $F(+)_x$ and E_{HOMO} could largely impact on adsorption behavior [56].

3.6. Degradation pathway of BPA

To further investigate the molecular characteristics of BPA, Fukui indices based on ·OH radical attack (F(0)) had been calculated using DFT method. Structural formula of BPA with atom number and Fukui function map were shown in Fig. 7. It was well accepted that the more F(0) value was, the more easily to be attacked by radicals [57]. As a result, the hydroxyl groups on the benzene rings could be replaced at first, and then C–C bond between the two aromatic rings would be attacked by oxidative reactive radical due to the high frontier electron density, therefore, two aromatic rings could separate from each other and generated phenol, isopropyl phenol, hydroquinone, benzoquinone, hydroxybenzoic acid and so on [58–60]. Thus, the substituent groups on the aromatic ring would further react with ·OH, which resulted in ring-open and then formed small molecular acids, such as oxalic acid, succinic acid and formic acid [59,61,62]. Finally, all these intermediates could be high-effectively mineralized into CO_2 and H_2O after CSCWO process. Based on these results, therefore, the conceivable degradation pathway of BPA was presented (Fig. 8). Firstly, ·OH would orderly attack the hydroxyl groups and the C–C bond between two aromatic rings according to the F(0) values. As a result, a series of intermediates generated, such as hydroquinone and phenols. Secondly, ·OH would further attack the substituent groups on the aromatic ring, which resulted in ring-open and then generated small molecular acids, like oxalic acid. At last, all these intermediates could be high-effectively mineralized into CO_2 and H_2O after CSCWO process.

4. Conclusion

The degradation of 18 aromatic compounds, containing aniline, quinoline, benzene, phenol, catechol, EDCs and so on, has been investigated under catalystic supercritical water oxidation process. The presence of catalysts, like Cu^{2+}, Fe^{3+}, Zn^{2+}, Ni^{2+}, Ag^{+}, Ce^{3+}, $Mn^{2+}$and Zr^{4+}, as well as PTA, TSA and PMA, could facilitate TOC removal. Among these catalysts, Cu(II) obtained the best TOC removal efficiency during CSCWO process. Additionally, TOC removal efficiencies of the aromatic compounds presented a sharp increase, as temperature and reaction time raised from 325 to 525 °C and from 0.5 to 6 min, respectively. The result of correlation analysis showed BO_n and $q(H)_x$ could largely impact the TOC degradation behaviors during CSCWO process. The conceivable degradation pathway of BPA was proposed, based on density functional theory (DFT) method. Firstly, the hydroxyl groups on the benzene rings could be attacked, and then C–C bond between the two aromatic rings would be broke via ·OH due to the high frontier electron density, as a result, two aromatic rings could separate from each other and generated a series of phenolic compounds. Secondly, the

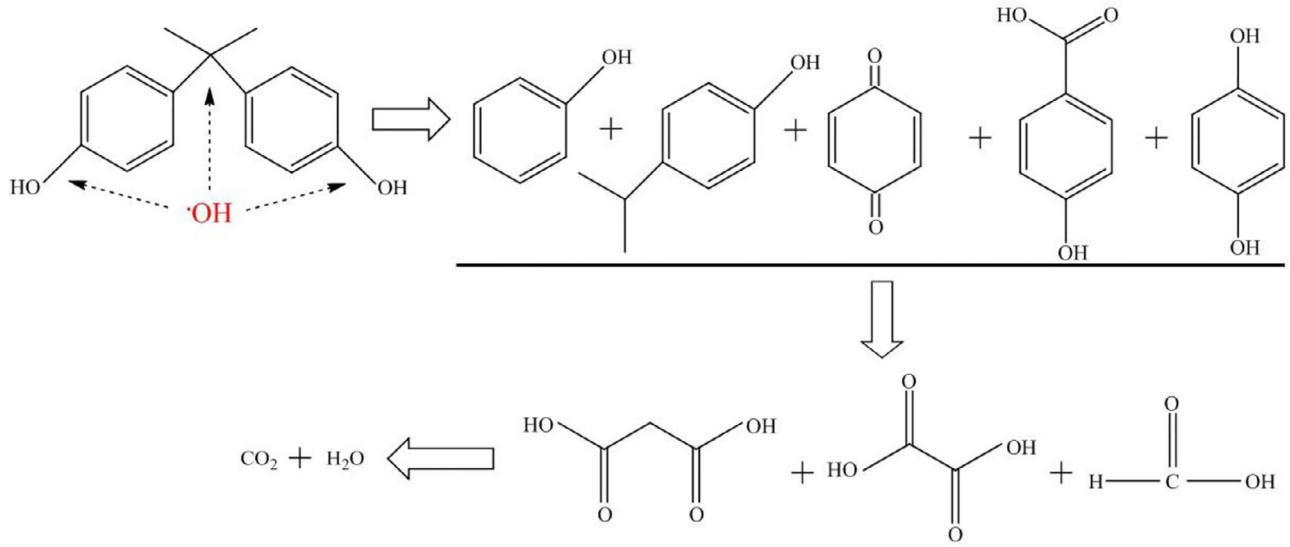

Fig. 8. The conceivable degradation pathways of BPA during CSCWO.

substituent groups on the aromatic ring would further react with ·OH, which resulted in ring-open and then formed small molecular acids. Finally, all these intermediates could be high-effectively mineralized into CO_2 and H_2O after CSCWO.

Acknowledgment

This work was supported by the NSFC project 21177083, NSFC key project 21537002, National water pollution control key project 2017ZX07202005-005.

Supplementary materials

Supplementary material associated with this article can be found, in the online version, at doi:10.1016/j.jtice.2019.02.002.

References

[1] Grung M, Kringstad A, Baek K, Allan IJ, Thomas KV, Meland S, Ranneklev SB. Identification of non-regulated polycyclic aromatic compounds and other markers of urban pollution in road tunnel particulate matter. J. Hazard. Mater. 2017;323:36–44.
[2] Johnson W, Idowu I, Francisco O, Marvin C, Thomas PJ, Stetefeld J, Tomy GT. Enumeration of the constitutional isomers of environmentally relevant substituted polycyclic aromatic compounds. Chemosphere 2018;202:9–16.
[3] Oishi Y. Comparison of moss and pine needles as bioindicators of transboundary polycyclic aromatic hydrocarbon pollution in central Japan. Environ. Pollut. 2018;234:330–8.
[4] Jiang C, Li S, Zhang P, Wang J. Pollution level and seasonal variations of carbonyl compounds, aromatic hydrocarbons and TVOC in a furniture mall in Beijing, China. Build. Environ. 2013;69:227–32.
[5] Goyak KO, Kung MH, Chen M, Aldous KK, Freeman JJ. Development of a screening tool to prioritize testing for the carcinogenic hazard of residual aromatic extracts and related petroleum streams. Toxicol. Lett. 2016;264:99–105.
[6] Rani M, Shanker U. Removal of carcinogenic aromatic amines by metal hexacyanoferrates nanocubes synthesized via green process. J. Environ. Chem. Eng. 2017;5:5298–311.
[7] Saal FS, Hughes C. An extensive new literature concerning low-dose effects of bisphenol a shows the need for a new risk assessment. Environ. Health Perspect. 2005;113:926–33.
[8] Bechambi O, Najjar W, Sayadi S. The nonylphenol degradation under UV irradiation in the presence of Ag–ZnO nanorods: effect of parameters and degradation pathway. J. Taiwan Inst. Chem. Eng. 2016;60:496–501.
[9] Porter KL, Olmstead AW, Kumsher DM, Dennis WE, Sprando RL, Holcombe GW, Korte JJ, Lindberg-Livingston A, Degitz SJ. Effects of 4-tert-octylphenol on Xenopus tropicalis in a long term exposure. Aquatic. Toxicol. 2011;103:159–69.
[10] Aivalioti M, Vamvasakis I, Gidarakos E. BTEX and MTBE adsorption onto raw and thermally modified diatomite. J. Hazard. Mater. 2010;178:136–43.
[11] Kümmerer K, Al-Ahmad AM-SV. Biodegradability of some antibiotics, elimination of the genotoxicity and affection of wastewater bacteria in a simple test. Chemosphere 2000;40:701–10.
[12] Qian L, Wang S, Xu D, Guo Y, Tang X, Wang L. Treatment of municipal sewage sludge in supercritical water: a review. Water Res 2016;89:118–31.
[13] Cocero MJ. Supercritical water processes: future prospects. J. Supercrit. Fluids 2018;134:124–32.
[14] Stavbar S, Hrnčič MK, Premzl K, Kolar M, Turk SŠ. Sub- and super-critical water oxidation of wastewater containing amoxicillin and ciprofloxacin. J. Supercrit. Fluids 2017;128:73–8.
[15] Pérez E, Fraga-Dubreuil J, García-Verdugo E, Hamley PA, Thomas WB, Housley D, Partenheimer W, Poliakoff M. Selective aerobic oxidation of para-xylene in sub- and supercritical water. Part 1. Comparison with ortho-xylene and the role of the catalyst. Green Chem. 2011;13:2389.
[16] Qi X, Zhuang Y, Yuan Y, Gu W. Decomposition of aniline in supercritical water. J. Hazard. Mater. 2002;90:51–62.
[17] Guo Y, Wang S, Yeh T, Savage PE. Catalytic gasification of indole in supercritical water. Appl. Catal. B 2015;166-167:202–10.
[18] Gong Y, Guo Y, Sheehan JD, Chen Z, Wang S. Oxidative degradation of landfill leachate by catalysis of CeMnO x /TiO 2 in supercritical water: mechanism and kinetic study. Chem. Eng. J. 2018;331:578–86.
[19] Golmohammadi M, Ahmadi SJ, Towfighi J. Catalytic supercritical water destructive oxidation of tributyl phosphate_ Study on the effect of operational parameters. J. Supercrit. Fluid 2018;140:32–40.
[20] Al-Duri B, Alsoqyani F. Supercritical water oxidation (SCWO) for the removal of nitrogen containing heterocyclic waste hydrocarbons. Part II: system kinetics. J. Supercrit. Fluid 2017;128:412–18.
[21] Dong X, Gan Z, Lu X, Jin W, Yu Y, Zhang M. Study on catalytic and non-catalytic supercritical water oxidation of p-nitrophenol wastewater. Chem. Eng. J. 2015;277:30–9.
[22] Shin YH, Lee H-s, Veriansyah B, Kim J, Kim DS, Lee HW, Youn Y-S, Lee Y-W. Simultaneous carbon capture and nitrogen removal during supercritical water oxidation. J. Supercrit. Fluid 2012;72:120–4.
[23] Esrafili MD, Mousavian P. Probing reaction pathways for oxidation of CO by O_2 molecule over P-doped divacancy graphene: a DFT study. Appl. Surf. Sci. 2018;440:580–5.
[24] Ai L, Zhou Y, Huang H, Lv Y, Chen M. A reactive force field molecular dynamics simulation of nickel oxidation in supercritical water. J. Supercrit. Fluid 2018;133:421–8.
[25] Wang R, Guo L, Jin H, Lu L, Yi L, Zhang D, Chen J. DFT study of the enhancement on hydrogen production by alkaline catalyzed water gas shift reaction in supercritical water. Int. J. Hydrogen Energy 2018.
[26] Tan Y, Shen Z, Guo W, Ouyang C, Jia J, Jiang W, Zhou H. Temperature sensitivity of organic compound destruction in SCWO process. J. Environ. Sci. 2014;26:512–18.
[27] Yang B, Shen Z, Cheng Z, Ji W. Total nitrogen removal, products and molecular characteristics of 14 N-containing compounds in supercritical water oxidation. Chemosphere 2017;188:642–9.
[28] Yang B, Cheng Z, Tang Q, Shen Z. Nitrogen transformation of 41 organic compounds during SCWO: a study on TN degradation rate, N-containing species distribution and molecular characteristics. Water Res. 2018;140:167–80.
[29] Ji W, Shen Z, Tang Q, Yang B, Fan M. A DFT study of Hg 0 adsorption on Co3O4 (1 1 0) surface. Chem. Eng. J. 2016;289:349–55.
[30] Cheng Z, Yang B, Chen Q, Gao X, Tan Y, Yuan T, Shen Z. Quantitative-structure-activity-relationship (QSAR) models for the reaction rate and temperature of nitrogenous organic compounds in supercritical water oxidation (SCWO). Chem. Eng. J. 2018;354:12–20.
[31] Park T-J, Lim JS, Lee Y-W, Kim S-H. Catalytic supercritical water oxidation of wastewater from terephthalic acid manufacturing process. J. Supercrit. Fluid 2003;26:201–13.
[32] Zhang Z, Baroutian S, Munir MT, Young BR. Variation in metals during wet oxidation of sewage sludge. Bioresour. Technol. 2017;245:234–41.
[33] Naeimi H, Zarabi MF. One pot synthesis of aminonaphthoquinone derivatives using Cu(II) immobilized on hyperbranched polyglycerol functionalized graphene oxide as a reusable catalyst under solvent-free conditions. Tetrahedron 2018;74:2314–23.
[34] Pérez E, Fraga-Dubreuil J, García-Verdugo E, Hamley PA, Thomas ML, Yan C, Thomas WB, Housley D, Partenheimer W, Poliakoff M. Selective aerobic oxidation of para-xylene in sub- and supercritical water. Part 2. The discovery of better catalysts. Green Chem. 2011;13:2397.
[35] Kosari M, Golmohammadi M, Towfighi J, Ahmadi SJ. Decomposition of tributhyl phosphate at supercritical water oxidation conditions: non-catalytic, catalytic, and kinetic reaction studies. J. Supercrit. Fluid 2018;133:103–13.
[36] Arslan I, Ferry J. HSiWO-catalyzed oxidation of nitrobenzene in supercritical water: kinetic and mechanistic aspects. Appl. Catal. B 2002;38:283–93.
[37] Fanning JC. The chemical reduction of nitrate in aqueous solution. Coord. Chem. Rev. 2000;199:159–79.
[38] Cox JL, Hallen RT, Lilga MA. Thermochemical nitrate destruction. Environ. Sci. Technol. 1994;28:423–8.
[39] Stutzenstein P, Weiner B, Köhler R, Pfeifer C, Kopinke F-D. Wet oxidation of process water from hydrothermal carbonization of biomass with nitrate as oxidant. Chem. Eng. J. 2018;339:1–6.
[40] Hatakeda K, Ikushima Y, Saito N, Liew C, Aizawa T. Corrosion on continuous supercritical water oxidation for polychlorinated biphenyls. High Pressure Res. 2001;20:393–401.
[41] Angeles-Hernández MJ, Leeke GA, Santos RCD. Catalytic supercritical water oxidation for the destruction of quinoline over MnO2/CuO mixed catalyst. Ind. Eng. Chem. Res. 2008;48:1208–14.
[42] Gao F, Li Y, Xiang B. Degradation of bisphenol A through transition metals activating persulfate process. Ecotoxicol. Environ. Saf. 2018;158:239–47.
[43] Potakis N, Frontistis Z, Antonopoulou M, Konstantinou I, Mantzavinos D. Oxidation of bisphenol A in water by heat-activated persulfate. J. Environ. Manage. 2017;195:125–32.
[44] Thomsen AB. Degradation of quinoline by wet air oxidation: kinetic aspects and reaction mechanisms. Water Res. 1998;32:136–46.
[45] Webley PA, Tester JW, Holgate HR. Oxidation kinetics of ammonia and ammonia -methanol mixtures in supercritical water in the temperature range 530-700 °C at 246 bar. Ind. Eng. Chem. Res. 1991;30:1745–54.
[46] Goto M, Nada T, Kodama A, Hirose T. Kinetic analysis for destruction of municipal sewage sludge and alcohol distillery wastewater by supercritical water oxidation. Ind. Eng. Chem. Res. 1999;38:1863–5.
[47] Segond N, Matsumura Y, Yamamoto K. Determination of ammonia oxidation rate in sub- and supercritical water. Ind. Eng. Chem. Res. 2002;41:6020–7.
[48] Mateos D, Portela JR, Mercadier J, Marias F, Marraud C, Cansell F. New approach for kinetic parameters determination for hydrothermal oxidation reaction. J. Supercrit. Fluid 2005;34:63–70.
[49] Nadjiba B, Nawel O, Abdesslam Hassen M. Modeling and optimization of phenol hydrothermal oxidation in supercritical water. Int. J. Hydrogen Energy 2017;42:12926–32.
[50] Portela JR, Nebo tE, Ossa EMDL. Kinetic comparison between subcritical and supercritical water oxidation of phenol. Chem. Eng. J. 2001;81:287–99.
[51] Tsipis AC. DFT challenge of intermetallic interactions: from metallophilicity and metallaromaticity to sextuple bonding. Coord. Chem. Rev. 2017;345:229–62.
[52] Ghasemi S, Noorizadeh S. Zero Steric Potential and bond order. Chem. Phys. Lett. 2016;652:106–11.
[53] Maridevarmath CV, Malimath GH. Computational and experimental studies on dielectric relaxation and dipole moment of some anilines and phenol. J. Mol. Liq. 2017;241:845–51.

[54] Fuentealba P, Florez ETW. Topological Analysis of the Fukui Function. J. Chem. Theory Comput. 2010;6:1470–8.
[55] Cheng Z, Yang B, Chen Q, Ji W, Shen Z. Characteristics and difference of oxidation and coagulation mechanisms for the removal of organic compounds by quantum parameter analysis. Chem. Eng. J. 2018;332:351–60.
[56] Su P, Zhu H, Shen Z. QSAR models for removal rates of organic pollutants adsorbed by in situ formed manganese dioxide under acid condition. Environ. Sci. Pollut. Res. Int. 2016;23:3609–20.
[57] Yang W, Mortier WJ. The use of global and local molecular parameters for the analysis of the gas-phase basicity of amines. Cheminform 1987;18:5708–11.
[58] Zhu H, Li Z, Yang J. A novel composite hydrogel for adsorption and photocatalytic degradation of bisphenol A by visible light irradiation. Chem. Eng. J. 2018;334:1679–90.
[59] Diao Z-H, Wei Q, Guo P-R, Kong L-J, Pu S-Y. Photo-assisted degradation of bisphenol A by a novel FeS 2 @SiO 2 microspheres activated persulphate process: synergistic effect, pathway and mechanism. Chem. Eng. J. 2018;349:683–93.
[60] Du J, Bao J, Liu Y, Ling H, Zheng H, Kim SH, Dionysiou DD. Efficient activation of peroxymonosulfate by magnetic Mn-MGO for degradation of bisphenol A. J. Hazard. Mater. 2016;320:150–9.
[61] Peng X, Tian Y, Liu S, Jia X. Degradation of TBBPA and BPA from aqueous solution using organo-montmorillonite supported nanoscale zero-valent iron. Chem. Eng. J. 2017;309:717–24.
[62] Xie Y, Li P, Zeng Y, Li X, Xiao Y, Wang Y, Zhang Y. Thermally treated fungal manganese oxides for bisphenol A degradation using sulfate radicals. Chem. Eng. J. 2018;335:728–36.